VIBRATION CHARACTERISTICS OF CFRP LAMINATES WITH EMBEDDED SHAPE MEMORY ALLOY FIBERS

Masaki Sato[1], Hideki Sekine[1], and Yuichi Hayakawa[1]

[1]*Department of Aeronautics and Space Engineering, Tohoku University*
Aramaki Aza Aoba 01, Aoba-ku, Sendai 980-8579, Japan

SUMMARY: The present paper examines vibration characteristics of symmetric CFRP laminates with embedded shape memory alloy fibers for passive vibration control by tailoring laminate configuration. The effect of recovery stresses induced by the embedded SMA fibers is taken into consideration in the free vibration analysis. With the use of two in-plane lamination parameters in addition to four out-of-plane lamination parameters, the shape memory effect on fundamental frequencies is discussed for the case of simply supported edges. The laminate configurations corresponding to six lamination parameters are also obtained by using a mathematical programming method. The results give a feasible region of two in-plane lamination parameters. By using two in-plane lamination parameters as design variables and the obtained feasible region as a constraint, the optimal laminate configurations to maximize the fundamental frequencies at the austenite phase are obtained.

KEYWORDS: Shape memory alloy fiber, Shape memory effect, CFRP, Symmetric laminate, Fundamental frequency, Vibration control, Laminate configuration, Lamination parameter.

INTRODUCTION

It is important to develop smart structures to meet various demands for future aerospace structures. In the development of the smart structures, shape memory alloys (SMA's) such as Ni-Ti alloys, are useful materials to give the structures numerous adaptive capabilities [1~3]. The SMA exhibits some unique characteristics. One of the most important characteristics is shape memory effect (SME). The SMA can deform plastically at a low-temperature martensite phase and then restore to the original shape by heating it above a proper transition temperature to an austenite phase. The other is the large change in the Young's modulus when the SMA transforms from the martensite phase to the austenite one [4].

The concept of smart composites using SMA was proposed by Rogers et al [5]. The modeling for SMA reinforced composite plates was shown and the structural control schemes were classified as active properties tuning and active strain energy tuning [6]. In the CFRP laminates with embedded SMA fibers, the recovery stresses induced by SMA fibers increase the vibration frequencies at the austenite phase [6,7]. Thus the vibration characteristics can be controlled by activating the embedded SMA fibers as actuators. In the vibration control of the laminates, not only active vibration control by activating the embedded SMA fibers but also passive vibration control by tailoring layer angles and layer thicknesses is important. The

laminates can be designed to have the most effective capability to increasing fundamental frequencies by passive vibration control.

In the design of composite laminates by tailoring laminate configuration, the lamination parameters are useful design variables [8,9]. Thus the present paper examines the vibration characteristics of symmetric CFRP laminates with embedded SMA fibers on the concept of lamination parameters. The SME on the fundamental frequencies has been investigated by using two in-plane lamination parameters in addition to four out-of-plane lamination parameters. Since the relationship among six lamination parameters have not been established so far, a mathematical programming method is applied to obtain the laminate configurations corresponding to six lamination parameters. The present paper also applies a mathematical programming method to obtain laminate configurations maximizing the fundamental frequencies at the austenite phase for passive vibration control.

FUNDAMENTAL EQATIONS

Model of CFRP Laminates with Embedded SMA Fibers

Figure 1 shows the model of the symmetric CFRP laminates with embedded SMA fibers. As shown in Fig. 1(a), the SMA fibers are embedded uniformly along the carbon fibers in each CFRP lamina with the volume fraction V_f. The material properties of this lamina can be expressed as follows, by using the rule-of-mixture:

$$
\begin{aligned}
E_1 &= E_{m1}\left(1-V_f\right)+E_f V_f \\
E_2 &= \frac{E_{m2}E_f}{E_{m2}V_f + E_f\left(1-V_f\right)} \\
G_{12} &= \frac{G_{m12}G_f}{G_{m12}V_f + G_f\left(1-V_f\right)} \\
\boldsymbol{n}_{12} &= \boldsymbol{n}_{m12}\left(1-V_f\right)+\boldsymbol{n}_f V_f \\
\boldsymbol{r} &= \boldsymbol{r}_m\left(1-V_f\right)+\boldsymbol{r}_f V_f
\end{aligned}
\tag{1}
$$

where subscripts " m " and " f ", respectively, denote the CFRP and the SMA fiber, while " 1 " and " 2 ", respectively, denote the direction of the fiber and the transverse direction to the fiber.

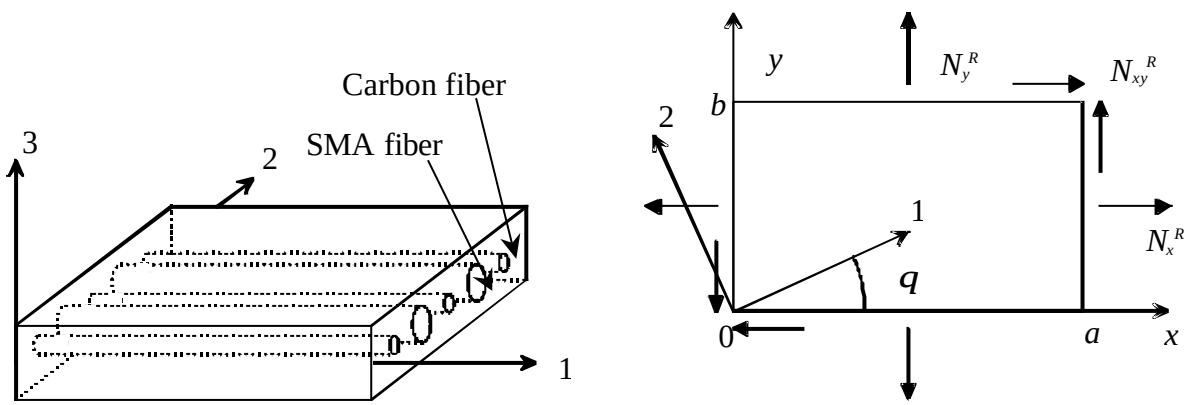

(a) Lamina model *(b) Symmetric laminate*

Fig. 1 : CFRP laminate with embedded SMA fibers

In the present lamina model shown in Fig. 1(a), we assume that the SMA fibers with initial plastic strain are embedded in each CFRP lamina. When any in-plane deformations of the lamina are restrained by the boundary condition at four edges, the embedded SMA fibers induce the recovery stresses along the fiber direction in the lamina. The induced recovery stresses in the lamina with layer angle θ can be expressed as follows:

$$\begin{Bmatrix} \sigma_x^R \\ \sigma_y^R \\ \sigma_{xy}^R \end{Bmatrix} = \begin{bmatrix} \cos^2\theta & \sin^2\theta & -2\sin\theta\cos\theta \\ \sin^2\theta & \cos^2\theta & 2\sin\theta\cos\theta \\ \sin\theta\cos\theta & -\sin\theta\cos\theta & \sin^2\theta \end{bmatrix} \begin{Bmatrix} \sigma^R V_f \\ 0 \\ 0 \end{Bmatrix} \tag{2}$$

where σ^R denotes the recovery stress of the SMA fiber. The directions shown in Fig. 1(b) represent the positive directions.

Lamination Parameters

In the classical laminate plate theory, the governing equation for free vibration of symmetric CFRP laminates with embedded SMA fibers, as shown in Fig. 1(b), is

$$\begin{aligned} D_{11}\frac{\partial^4 w}{\partial x^4} + 4D_{16}\frac{\partial^4 w}{\partial x^3 \partial y} + 2(D_{12}+2D_{66})\frac{\partial^4 w}{\partial x^2 \partial y^2} + 4D_{26}\frac{\partial^4 w}{\partial x \partial y} + D_{22}\frac{\partial^4 w}{\partial y^4} \\ - N_x^R \frac{\partial^2 w}{\partial x^2} - N_y^R \frac{\partial^2 w}{\partial y^2} - 2N_{xy}^R \frac{\partial^2 w}{\partial x \partial y} = \rho h \omega^2 w \end{aligned} \tag{3}$$

where w, ρ, h and ω denote the deflection, density and thickness of the plate and the circular frequency, respectively. Introducing stiffness invariants U_i and lamination parameters ξ_i, the out-of-plane stiffnesses can be expressed as follows [10]:

$$\begin{Bmatrix} D_{11} \\ D_{22} \\ D_{12} \\ D_{66} \\ D_{16} \\ D_{26} \end{Bmatrix} = \frac{h^3}{12} \begin{bmatrix} 1 & \xi_9 & \xi_{10} & 0 & 0 \\ 1 & -\xi_9 & \xi_{10} & 0 & 0 \\ 0 & 0 & -\xi_{10} & 1 & 0 \\ 0 & 0 & -\xi_{10} & 0 & 1 \\ 0 & \xi_{11}/2 & \xi_{12} & 0 & 0 \\ 0 & \xi_{11}/2 & -\xi_{12} & 0 & 0 \end{bmatrix} \begin{Bmatrix} U_1 \\ U_2 \\ U_3 \\ U_4 \\ U_5 \end{Bmatrix} \tag{4}$$

The recovery stress resultants can be written as follows:

$$\begin{Bmatrix} N_x^R \\ N_y^R \\ N_{xy}^R \end{Bmatrix} = h\int_0^1 \begin{Bmatrix} \sigma_x^R \\ \sigma_y^R \\ \sigma_{xy}^R \end{Bmatrix} du = \frac{h}{2}\sigma_r V_f \begin{Bmatrix} 1+\xi_1 \\ 1-\xi_1 \\ \xi_3 \end{Bmatrix} \tag{5}$$

It should be noted that the recovery stress resultants are only related to SME. If the embedded SMA fibers are not activated, SME has no contribution to the recovery stress resultants, because σ^R=0 at the martensite phase. Lamination parameters are written as follows, with a symmetric condition at the mid-plane:

$$(\xi_1, \xi_2, \xi_3, \xi_4) = \int_0^1 (\cos 2\theta, \cos 4\theta, \sin 2\theta, \sin 4\theta)\, du \tag{6}$$

$$(\xi_9, \xi_{10}, \xi_{11}, \xi_{12}) = 3\int_0^1 (\cos 2\theta, \cos 4\theta, \sin 2\theta, \sin 4\theta) u^2\, du \tag{7}$$

where $q(u)$ is a distribution function of fiber orientation angles through the thickness and $u(=2z/h)$ is a non-dimensional thickness. When the layer angle distribution is specified through the thickness, the lamination parameters can be determined uniquely. In Eqns 6 and 7, (x_1,x_2,x_3,x_4) and $(x_9,x_{10},x_{11},x_{12})$ represent the in-plane and the out-of-plane lamination parameters, respectively.

From Eqns 3, 4 and 5, the vibration characteristics at the austenite phase are governed by six lamination parameters $(x_1,x_3,x_9,x_{10},x_{11},x_{12})$ with taking the recovery stress resultants into consideration. On the contrary, the vibration characteristics at the martensite phase are governed by only four lamination parameters $(x_9,x_{10},x_{11},x_{12})$. It is known that the lamination parameters are not independent. The relationship among the four in-plane or the four out-of-plane lamination parameters was obtained in Ref. 8. In Ref. 9, a method to determine the laminate configurations from the specified in-plane or out-of-plane lamination parameters is also suggested. But the relationship among the six lamination parameters $(x_1,x_3,x_9,x_{10},x_{11},x_{12})$ has not been established. Thus the method to determine the laminate configurations corresponding to six lamination parameters has not been provided yet.

Vibration Analysis

We examine the fundamental frequencies of the CFRP laminates with embedded SMA fibers as shown in Fig. 1. The laminate is simply supported at four edges. The boundary conditions for simply supported edges are expressed as follows:

$$\begin{aligned} x=0,a\ ;\ w&=D_{11}\frac{\partial^2 w}{\partial x^2}+D_{12}\frac{\partial^2 w}{\partial y^2}+2D_{16}\frac{\partial^2 w}{\partial x\partial y}=0 \\ y=0,b\ ;\ w&=D_{12}\frac{\partial^2 w}{\partial x^2}+D_{22}\frac{\partial^2 w}{\partial y^2}+2D_{26}\frac{\partial^2 w}{\partial x\partial y}=0 \end{aligned} \tag{8}$$

The following deflection function is assumed:

$$w(x,y)=\sum_{m=1}^{M}\sum_{n=1}^{N}A_{mn}\sin\frac{m\pi x}{a}\sin\frac{n\pi y}{b} \tag{9}$$

The deflection function does not satisfy the natural boundary condition, and hence, we use the Rayleigh-Ritz method. Applying the Rayleigh-Ritz method, we can obtain a eigenvalue equation. The second power of fundamental frequency is given as the positive lowest eigenvalue. The fundamental frequency is normalized as follows:

$$\bar{\omega}^2=\frac{12b^4\rho_m}{\pi^4 Q_{m22}h^2}\omega^2 \tag{10}$$

where Q_{m22} is the reduced stiffness transverse to the fiber. The increasing rate of normalized vibration frequencies is defined as follows:

$$D\bar{\omega}=\frac{\bar{\omega}_A-\bar{\omega}_M}{\bar{\omega}_M}\times 100\ \ (\%) \tag{11}$$

where $\bar{\omega}_M$ and $\bar{\omega}_A$ denote the normalized fundamental frequencies at the martensite phase and at the austenite phase, respectively.

SHAPE MEMORY EFFECT ON VIBRATION CHARACTERISTICS

As a numerical example, we consider graphite/epoxy composites as the CFRP and Ni-Ti alloys as the embedded SMA fibers. The material properties of graphite/epoxy composites are

$$E_{m1} = 148.0 \text{ GPa},\ E_{m2} = 10.8 \text{ GPa},\ G_{m12} = 5.49 \text{ GPa},\ \nu_{m12} = 0.3. \tag{12}$$

The material properties of Ni-Ti alloys [4] are

$$\begin{aligned} &\text{at martensite phase}\ ;\ E_f = 27.6 \text{ GPa},\ G_f = 10.4 \text{ GPa},\ \nu_f = 0.33,\ \sigma^R = 0.0 \text{ GPa} \\ &\text{at austenite phase}\ ;\ E_f = 82.7 \text{ GPa},\ G_f = 31.1 \text{ GPa},\ \nu_f = 0.33,\ \sigma^R = 0.138 \text{ GPa} \end{aligned} \tag{13}$$

and the volume fraction of the SMA fiber is assumed as V_f=0.15.

Figure 2 shows the contours of the increasing rates of normalized fundamental frequencies $D\overline{\omega}$ on the in-plane lamination parameters plane x_1-x_3 within the region of $x_1^2 + x_3^2 \le 1$. In Figs. 2(a), 2(b) and 2(c), the contours are shown for the case of (x_9,x_{10},x_{11},x_{12})=(0,-1,0,0), (0,0,0,0) and (0,1,0,0). Those out-of-plane lamination parameters define the out-of-plane stiffnesses of the $\pm 45^\circ$ angle-ply laminates, the isotropic laminates and the $0^\circ / 90^\circ$ cross-ply laminates, respectively, and $x_1^2 + x_3^2 \le 1$ shows the feasible region of (x_1,x_3) without no contribution of (x_9,x_{10},x_{11},x_{12}) [8]. The aspect ratio of the laminate is a/b=1. From those figures we can know the SME on the fundamental frequencies. In any figures, the fundamental frequencies at the austenite are increased by SME compared with those at the martensite phase. The maximum $D\overline{\omega}$ appears on the x_1-axis. It means that the fundamental frequencies at the austenite phase are most increased when the recovery stress resultants condition is N_{xy}^R=0. It can be also known the increasing rates of the normalized fundamental frequencies of the cross-ply laminates are highest among the three laminates.

DETERMINATION OF LAMINATE CONFIGURATIONS CORRESPONDING TO SIX LAMINATION PARAMETERS

When we discuss the vibration characteristics of the CFRP laminate with embedded SMA fibers with use of six lamination parameters, we need determine the corresponding laminate configurations. In this section, we will obtain the laminate configurations corresponding to six lamination parameters by using a mathematical programming method.

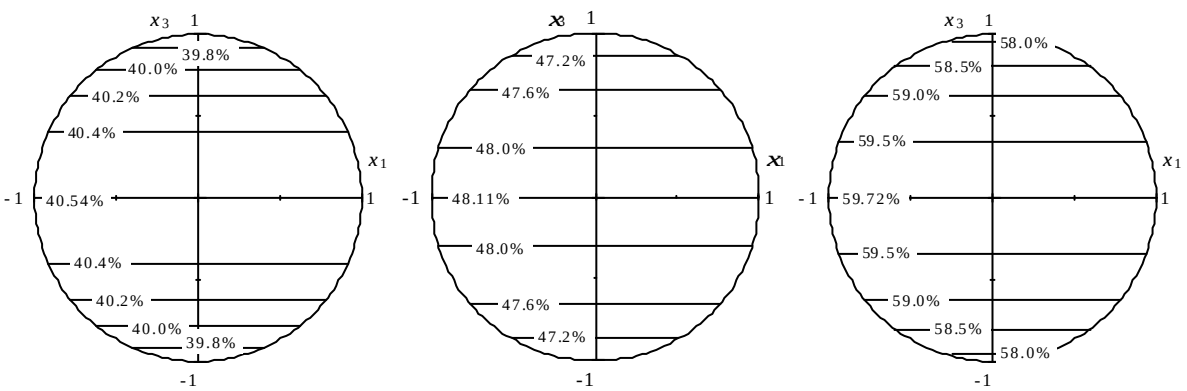

(a) (x_9,x_{10},x_{11},x_{12})=(0,-1,0,0) (b) (x_9,x_{10},x_{11},x_{12})=(0,0,0,0) (c) (x_9,x_{10},x_{11},x_{12})=(0,1,0,0)

Fig. 2 : Contours of $D\overline{\omega}$ on x_1-x_3 plane (a/b=1.0)

Problem Formulation

We consider the following optimization problem to obtain the laminate configurations corresponding to specified six lamination parameters x_i. The optimization problem can be stated as follows:

$$\begin{aligned} &\text{minimize} && \Delta x = \sum_{i=1,3,9\sim12} W_i \left(x_i - x_i^*\right)^2 \\ &\text{design variables} && \theta_k \ , \ h_k \ \left(k = 1 \sim N\right) \end{aligned} \tag{14}$$

where x_i^* denote the lamination parameters realized by $2N$-layered symmetric laminates consisted of layer angles θ_k and layer thicknesses h_k, and W_i denotes the weight function. When the layer angles θ_k and the layer thicknesses h_k that give zero to the value of Δx are obtained, the laminate configurations corresponding to specified six lamination parameters are realized. As an optimizer, the BFGS method was adopted with the golden section method in ADS program [11].

Numerical Results and Discussions

As an numerical example, three sets of specified lamination parameters are used to obtain the corresponding laminate configurations: case 1, $(x_1,x_3,x_9,x_{10},x_{11},x_{12})=(0,0,0,-1,0,0)$; case 2, $(x_1,x_3,x_9,x_{10},x_{11},x_{12})=(0,0.5,0,-1,0,0)$; case 3, $(x_1,x_3,x_9,x_{10},x_{11},x_{12})=(0,1,0,-1,0,0)$. Those sets of lamination parameters are corresponding to the points on the x_1-axis in Fig. 2(a), which give the maximum $\Delta\overline{w}$. In the optimization, the weight function is W_i=1 and one thousand sets of initial values generated by a random number generator are used to obtain the reliable results.

Table 1 shows the optimal results for case 1. The minimized values of Δx are shown for the $2N$-layered symmetric laminates. The laminate configurations to minimize Δx and realized lamination parameters x_i^* by the $2N$-layered symmetric laminates are also shown in Table 1. When the number of layers is $2N$=2 or 4, the minimized value of Δx is not zero and the obtained laminate configurations can not realize the specified six lamination parameters. On the contrary, the obtained laminate configurations for $2N$=6 and 8 can realize the specified six lamination parameters with the values of Δx=0.

Table 1 : Optimal laminate configurations to minimize Δx for $(x_1,x_3,x_9,x_{10},x_{11},x_{12})=(0,0,0,-1,0,0)$

$2N$	Δx	Laminate configurations					
		x_1^*	x_3^*	x_9^*	x_{10}^*	x_{11}^*	x_{12}^*
2	2.0000	$[-45.0^\circ{}_{1.00}]_S$					
		0.00	-1.00	0.00	-1.00	-1.00	0.00
4	0.2571	$[45.0^\circ{}_{0.29}/-45.0^\circ{}_{0.71}]_S$					
		0.00	-0.42	0.00	-1.00	0.29	0.00
6	0.0000	$[45.0^\circ{}_{0.19}/-45.0^\circ{}_{0.50}/45.0^\circ{}_{0.31}]_S$					
		0.00	0.00	0.00	-1.00	0.00	0.00
8	0.0000	$[45.2^\circ{}_{0.09}/-45.0^\circ{}_{0.27}/44.8^\circ{}_{0.41}/-45.3^\circ{}_{0.23}]_S$					
		0.00	0.00	0.00	-1.00	0.00	0.00

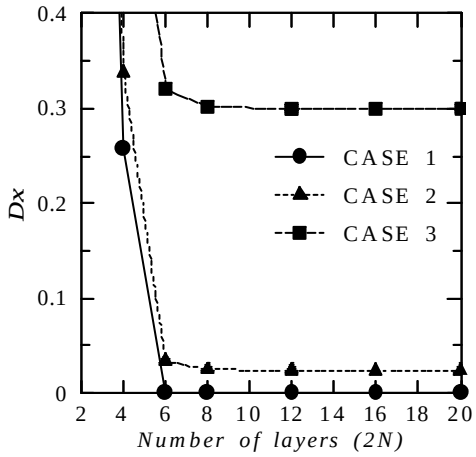

Fig.3 : Convergence behavior of Δx

Figure 3 shows the convergence behavior of Dx with the number of layers $2N$. In case 1, the values of Dx are converged to zero when the number of layers $2N$ is more than 6. On the contrary, the values of Dx do not became zero in case 2 and case 3. Thus the specified lamination parameters in case 1 are realized by the symmetric laminates consist of more than 6 layers, while the specified laminate parameters in case 2 and case 3 can not be realized even if the 20-layered symmetric laminates are used.

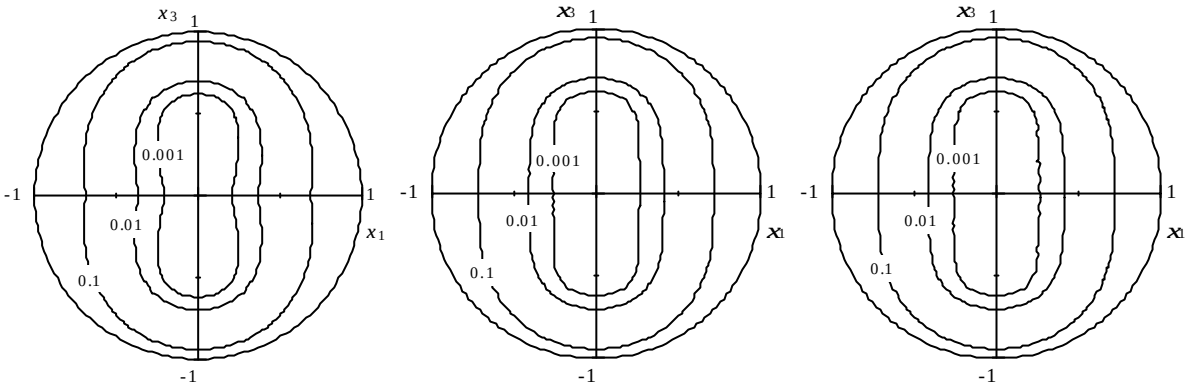

(a) 6-layered symmetric laminates (2N=6) *(b) 8-layered symmetric laminates (2N=8)* *(c) 20-layered symmetric laminates (2N=20)*

Fig. 4 : Contours of Dx on x_1-x_3 plane for $(x_9,x_{10},x_{11},x_{12})=(0, -1, 0, 0)$

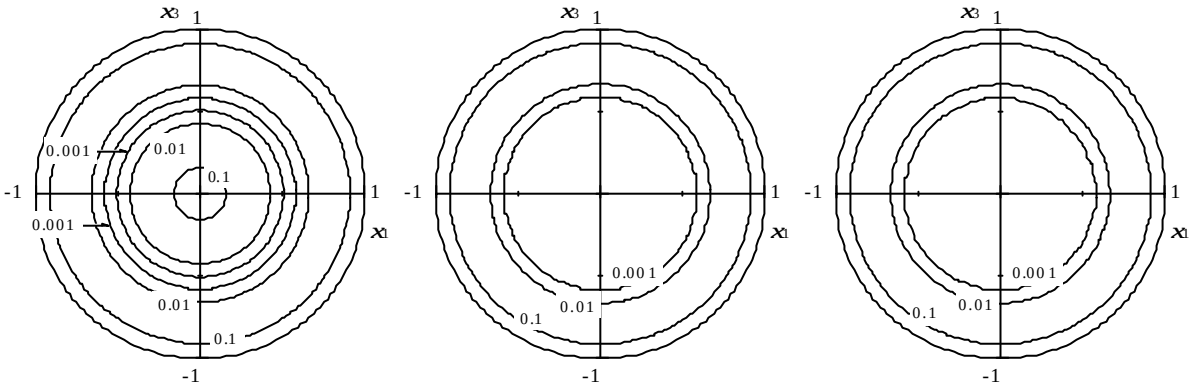

(a) 6-layered symmetric laminates (2N=6) *(b) 8-layered symmetric laminates (2N=8)* *(c) 20-layered symmetric laminates (2N=20)*

Fig. 5 : Contours of Dx on x_1-x_3 plane for $(x_9,x_{10},x_{11},x_{12})=(0, 0, 0, 0)$

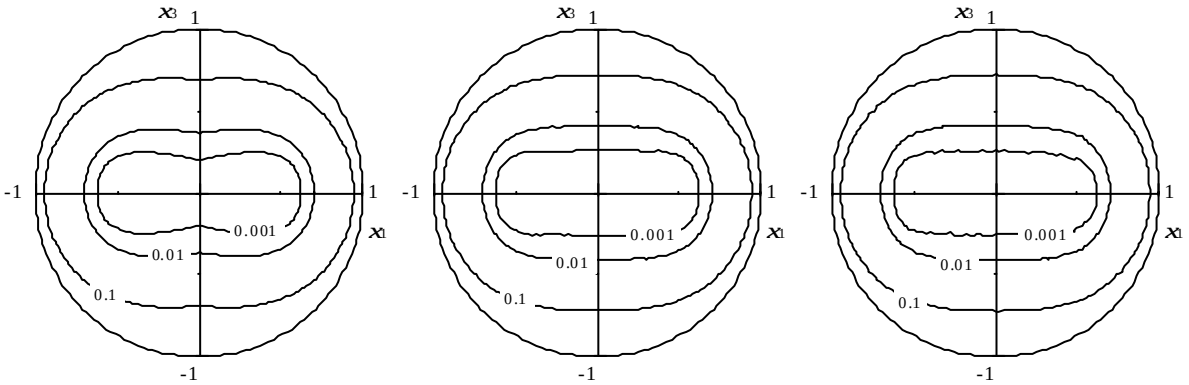

(a) 6-layered symmetric laminates (2N=6) *(b) 8-layered symmetric laminates (2N=8)* *(c) 20-layered symmetric laminates (2N=20)*

Fig. 6 : Contours of Dx on x_1-x_3 plane for $(x_9,x_{10},x_{11},x_{12})=(0, 1, 0, 0)$

Figures 4, 5 and 6 show the contours of Dx on the in-plane lamination parameters plane x_1-x_3 for the specified out-of-plane lamination parameters. In Fig. 4, Fig. 5 and Fig. 6, the contours are shown for $(x_9,x_{10},x_{11},x_{12})$=(0,-1,0,0), (0,0,0,0) and (0,1,0,0), respectively. Here, the number of layers is considered for the case of $2N$=6, 8 and 20. From those figures, we can know the feasible region of (x_1,x_3) for the specified $(x_9,x_{10},x_{11},x_{12})$. The feasible regions with taking the contribution of $(x_9,x_{10},x_{11},x_{12})$ into consideration are much limited than $x_1^2 + x_3^2 \le 1$. Comparing Fig. 4, 5 and 6, it is known that the feasible regions are depend on the specified $(x_9,x_{10},x_{11},x_{12})$. It can be also seen that the feasible regions are depend on the number of layers and the 8-layered symmetric laminates are enough to express the maximum feasible regions.

OPTIMIZATION OF VIBRATION CHARACTERISTICS

In this section, we will obtain the laminate configurations to maximize the fundamental frequencies at the austenite phase by using a mathematical programming method.

Problem Formulation

We consider an optimal design of the CFRP laminates with embedded SMA fibers that will provide the maximum fundamental frequencies at the austenite phase. Two in-plane lamination parameters x_1 and x_3 are used as design variables. Since the positive feasible region of (x_1,x_3) has not been provided, the mathematical results obtained in the former section are used as a constraint.

The optimization problem can be stated as follows when the fundamental frequencies at martensite phase are defined by specified four out-of-plane lamination parameters:

$$\begin{array}{ll} \text{maximize} & \Delta\overline{w}(x_1,x_3) \\ \text{design variables} & x_1,x_3 \\ \text{subject to} & \Delta x = 0 \end{array} \tag{15}$$

where Dx=0 denotes the feasible regions of (x_1,x_3) for the specified $(x_9,x_{10},x_{11},x_{12})$. As an optimizer, the modified feasible direction method was adopted with the golden section method in the ADS program [11].

In the optimization procedure, we will solve two optimization problems. One is the optimization problem to maximize $D\overline{w}$ and another is optimization problem to minimize Dx. The optimization problem to minimize Dx is solved as an auxiliary problem to obtain the information about the feasible region of in-plane lamination parameters. By linking the auxiliary optimization problems, we can solve the principal optimization problem stated in Eqn 15.

Numerical Results and Discussions

As a numerical example, the material properties specified in Eqns 12 and 13 are used. A laminate is simply supported at four edges. The aspect ratio of the laminate is a/b=1.

The effect of initial design variables on the optimal results have also been examined. The four sets of in-plane lamination parameters (x_1,x_3) were used as initial design variables: (x_1,x_3)= (1.0,0.0), (-1.0,0.0), (0.0,1.0) and (0.0,-1.0).

The optimal results for the case of (x_9,x_{10},x_{11},x_{12})=(0,-1,0,0), (0,0,0,0) and (0,1,0,0) are shown in Table 2. The numbers of layers are considered for the case of $2N$=6, 8 and 20. In any case, the optimal $D\overline{w}$ converged to almost the same values with the constraint Dx=0 independently of the initial in-plane lamination parameters. The appropriateness of the obtained optimal results is also confirmed by Fig. 2 and Figs. 4~6. Thus the present optimization approach with linking the auxiliary optimization problems is useful to solve the optimal problem with the unknown constraint. The laminate configurations corresponding to the optimal lamination parameters are shown in Table 3. In general, there exist an infinite number of laminate configurations to the same lamination parameters, since the stacking sequence of the laminate can vary arbitrary. An example of laminate configurations is shown for 6-layered symmetric laminates.

CONCLUSIONS

The SME on the fundamental frequencies has been investigated by using six lamination parameters for the symmetric CFRP laminates with embedded SMA fibers. It has been shown that the fundamental frequencies at the austenite phase are increased by SME of embedded SMA fibers. By representing the increasing rates of the normalized fundamental frequencies on the in-plane lamination parameters plane, the most effective recovery stress resultants conditions are clarified. The laminate configurations corresponding to six lamination parameters are obtained by a mathematical programming method. The results gives us not only the laminate configurations but also the feasible region of (x_1,x_3) for the specified (x_9,x_{10},x_{11},x_{12}), which has not been known so far. When the specified (x_9,x_{10},x_{11},x_{12}) is taken into consideration, the feasible regions of (x_1,x_3) are much limited compared with those leaving them out of consideration. The optimal laminate configurations to maximize the

Table 2 : Optimal in-plane lamination parameters and $D\overline{w}$

Specified out-of-plane lamination parameters				$2N$	Optimal in-plane lamination parameters		Dx	$D\overline{w}$
x_9	x_{10}	x_{11}	x_{12}		x_1	x_3		
0.00	-1.00	0.00	0.00	6	0.00	0.00	0.0000	40.54
				8	0.00	0.00	0.0000	40.54
				20	-0.03	0.01	0.0000	40.54
0.00	0.00	0.00	0.00	6	-0.54	0.00	0.0000	48.11
				8	-0.01	-0.01	0.0000	48.11
				20	0.00	0.00	0.0000	48.11
0.00	1.00	0.00	0.00	6	0.00	0.00	0.0000	59.72
				8	0.00	0.00	0.0000	59.72
				20	-0.17	0.01	0.0000	59.72

Table 3 : Optimal laminate configurations (2N=6)

Lamination parameters						Laminate configurations
x_1	x_3	x_9	x_{10}	x_{11}	x_{12}	
0.00	0.00	0.00	-1.00	0.00	0.00	$[-45.0^\circ{}_{0.19}/45.0^\circ{}_{0.50}/-45.0^\circ{}_{0.31}]_S$
-0.54	0.00	0.00	0.00	0.00	0.00	$[-27.5^\circ{}_{0.13}/32.4^\circ{}_{0.18}/-87.5^\circ{}_{0.69}]_S$
0.00	0.00	0.00	1.00	0.00	0.00	$[0.0^\circ{}_{0.19}/90.0^\circ{}_{0.50}/0.0^\circ{}_{0.31}]_S$

fundamental frequencies at the austenite phase are also obtained by using a mathematical programming method. In the optimization, an auxiliary optimization problem is linked to obtain the feasible regions of (x_1, x_3). The present optimization approach is useful for the optimization problems with unknown constraint. Since the optimal laminate configurations obtained by this approach have the most effective capability to maximize the fundamental frequencies at austenite phase, they are useful laminate configurations for passive vibration control.

REFERENCES

1. Fuller, C. R., Rogers, C. A. and Robertshaw, H. H., "Control of Sound Radiation With Active/Adaptive Structures", *Journal of Sound and Vibration*, Vol. 157, No. 1, 1992, pp. 19-39.

2. Furuya, Y., Sasaki, A. and Taya, M., "Enhanced Mechanical Prorpeties of TiNi Shape Memory Fiber / Al Matrix Composite", *Materials Transactions*, JIM, Vol. 34, No. 3, 1993, pp. 224-227.

3. Choi, S. and Lee, J. J., "The Shape Control of Composite Beam With Embedded Shape Memory Alloy Wire Actuators", *Smart Materials and Structures*, Vol. 7, 1998, pp. 759-770.

4. Jackson, C. M., Wagner, H. J. and Wasilewski, R. J., "55-Nitinol – The Alloy with A Memory: Its Physical Metallurgy, Properties, and Applications", *NASA-SP 5110*, 1972

5. Rogers, C. A., Liang, C. and Jia, J., "Behavior of Shape Memory Alloy Reinforced Composite Plates Part I: Model Formulations and Control Concepts", *American Institute of Aeronautics and Astronautics Paper 89-1389*, 1989, pp. 2011-2017.

6. Liang, C., Jia, J. and Rogers, C. A., "Behavior of Shape Memory Alloy Reinforced Composite Plates Part II: Results", *American Institute of Aeronautics and Astronautics Paper 89-1331*, 1989, pp. 1504-1513.

7. Epps, J. and Chandra, R., "Shape Memory Alloy Actuation for Active Tuning of Composite Beams", Smart Materials and Structures, Vol. 6, 1997, pp. 251-264.

8. Fukunaga, H. and Sekine, H., "Stiffness Design Method of Symmetric Laminates Using Lamination Parameters", *American Institute of Aeronautics and Astronautics Journal*, Vol. 30, No. 11, 1992, pp. 2791-2793.

9. Fukunaga, H. and Sekine, H., "A Laminate Design for Elastic Properties of Symmetric Laminates with Extension-Shear or Bending-Twisting Coupling", *Journal of Composite Materials*, Vol. 28, No.8, 1984, pp. 708-731.

10. Tsai, S. W. and Hahn, H. T., *Introduction to Composite Materials*, Technomic, Lancaster, PA, 1980

11. Vanderplaats, G. N. and Sugimoto, H., "A General Purpose Optimization Program for Engineering Design", *Computers & Structures*, Vol. 24, No. 1, 1986, pp. 13-21.